PAPER

Robust Moving Object Extraction and Tracking Method Based on Matching Position Constraints

Tetsuya OKUDA[†a)], *Nonmember*, Yoichi TOMIOKA[††b)], *Member*, *and* Hitoshi KITAZAWA[†c)], *Fellow*

SUMMARY Object extraction and tracking in a video image is basic technology for many applications, such as video surveillance and robot vision. Many moving object extraction and tracking methods have been proposed. However, they fail when the scenes include illumination change or light reflection. For tracking the moving object robustly, we should consider not only the RGB values of input images but also the shape information of the objects. If the objects' shapes do not change suddenly, matching positions on the cost matrix of exclusive block matching are located nearly on a line. We propose a method for obtaining the correspondence of feature points by imposing a matching position constraint induced by the shape constancy. We demonstrate experimentally that the proposed method achieves robust tracking in various environments.
key words: *moving object extraction, tracking, shape information, motion segmentation*

1. Introduction

For many applications in which video image analysis is implemented, such as video surveillance and robot vision, object extraction and tracking is a basic requirement. In particular, to achieve action recognition, it is necessary to obtain a detailed motion vector between consecutive frames. Many motion vector extraction methods have been proposed: Horn-Schunk [1], Lucas-Kanade [2], SIFT feature tracking [3], and exclusive block matching [4]. However, it is impossible to obtain the flow that constitutes the correspondence of feature points accurately using only appearance information. The appearance of an object can vary because of illumination changes or light reflection as it moves, as shown in Fig. 1. Moreover, if an area of an object is uniform in color, the extracted flows on the object can intersect each other. Therefore, we should consider the shape information when obtaining the correspondence of feature points.

In order to maintain shape constancy, several methods that minimize the energy function expressed by Eq. (1) have been proposed.

$$E = \sum_{p} d(p, p') + \lambda \sum_{p,q} s(p, p', q, q'). \quad (1)$$

Here, p and q are feature points in the current frame and p' and q' are those in the previous frame, which are matched with p and q, respectively. The similarity is calulated from the data term $[d(p, p')]$ and smoothness term $[s(p, p', q, q')]$. The former represents visual feature similarity, and the latter represents the shape similarity [5]. We can obtain the correspondences of the blocks by solving the minimization problem in Eq. (1) [6]. However, this problem cannot be solved strictly because we have to solve the quadratic assignment problem. Therefore, it is approximated by using the steepest descent method [7], a genetic algorithm (GA) [8], successive convexification [9], and the iteration of visual feature optimization and shape optimization [5].

In this study, we propose a new method for robustly obtaining the correspondence of feature points by applying matching position constraints on a cost matrix when the object shape does not change suddenly. Moreover, we show a condition of the object translation and rotation that allows us to consider the matching position on a line.

In the next section, we explain exclusive block matching as a basis for the proposed method. In Sect. 3, we introduce a theory for the alignment of matching positions. In Sect. 4, we describe a method for applying the matching position constraint for exclusive block matching. In Sect. 5, we show the experimental results of flow extraction and compare them with those of previous methods.

2. Exclusive Block Matching [4]

We explain the exclusive block matching method, which is a basic component of the proposed method. Exclusive block matching is a method of detecting the flow by obtaining the correspondence of the blocks between two successive frames; the procedures of exclusive block matching are summarized in Fig. 2. First, we divide the images of the pre-

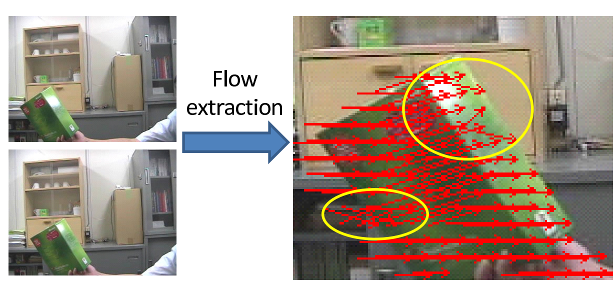

Fig. 1 Incorrect flow extraction by utilizing only color information.

Manuscript received September 3, 2014.
Manuscript revised March 17, 2015.
Manuscript publicized April 28, 2015.
[†]The authors are with the Tokyo University of Agriculture and Technology, Koganei-shi, 184–8588 Japan.
[††]The author is currently with the University of Aizu, Aizu-Wakamatsu-shi, 965–8580 Japan.
a) E-mail: 50013645206@st.tuat.ac.jp
b) E-mail: ytomioka@u-aizu.ac.jp
c) E-mail: kitazawa@cc.tuat.ac.jp
DOI: 10.1587/transinf.2014EDP7298

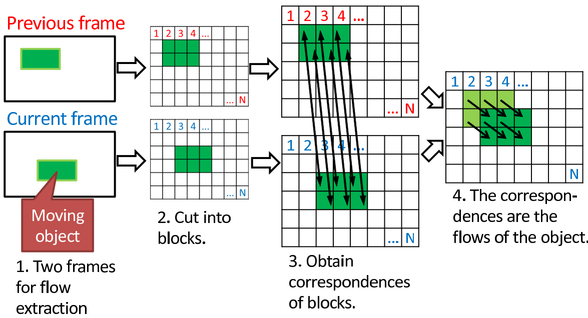

Fig. 2 Procedures of exclusive block matching.

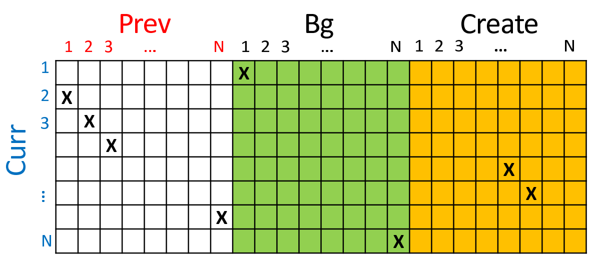

Fig. 3 Cost matrix extended for background and new object appearance. Each × denotes the matching position.

vious frame and the current frame into blocks of 8×8 pixels. Then, we generate a cost matrix by calculating the similarity between the current and previous frame's blocks. We extend the cost matrix as shown in Fig. 3 for matching to the background image (Bg) and appearance of the new object (Create). A current frame's block that resembles background image block matches a diagonal element of Bg matrix. HSV histogram and HOG [10] are employed as the feature of each block, and the Bhattacharyya distance is employed for calculating the similarity. The optimum correspondence of the block is determined such that the total cost is minimized, by solving the linear assignment problem.

3. Alignment of Matching Positions

For each motion of an object, the matching positions of a cost matrix, as shown in Fig. 3, are arranged in a certain pattern depending on the motion. In particular, when the object shape is not changed significantly and the translation and rotation are small, the matching points are arranged approximately in a certain line, as shown in Fig. 4. By using this matching position constraint, robust tracking can be achieved. In this section, we analyze the patterns of matching positions for basic movements: translation and rotation.

For a cost matrix, the row index i represents the i-th block of the current frame in raster scanning order. Similary, the column index j represents the j-th block of the previous frame. When the i-th block of the current frame is matched with the j-th block of the previous frame, element $c(i, j)$ is a matching position on the cost matrix. An object can be deemed to consist of some blocks, and they move together while the object moves. For example, when an object is magnified, as shown in Fig. 5 (a), the matching positions of

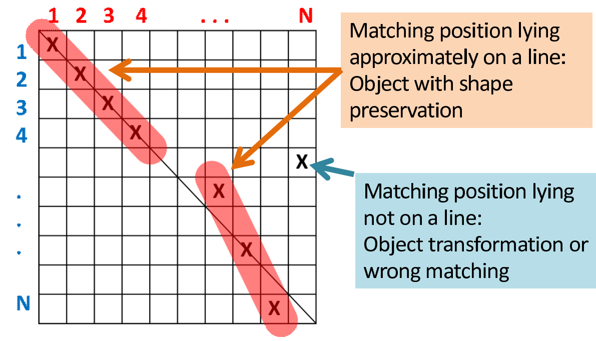

Fig. 4 Alignment of matching positions on a cost matrix.

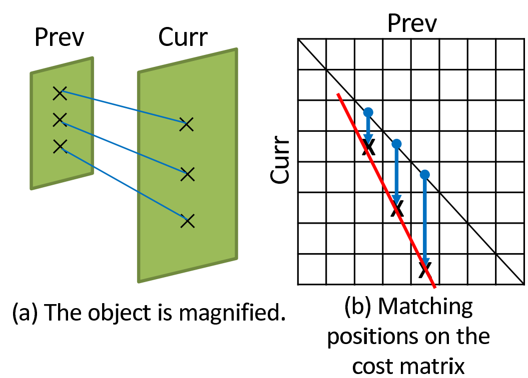

Fig. 5 Matching positions on the cost matrix form a figure.

the blocks, indicated by "×" in Fig. 5 (a), are arranged in a line on the cost matrix, as shown in Fig. 5 (b). It should be noted that this line appears not on the screen but on the cost matrix.

Since the matching positions are sparse on the cost matrix, we convert the cost matrix by collecting them in the compartment of the upper left hand corner of the cost matrix to facilitate understanding that the matching positions are arranged in a certain figure. The collected matching pattern depends on the block scanning direction for generating the initial cost matrix. The cost matrix generated by raster scanning in the X-Y (Y-X) direction, as shown in Fig. 6, is called X-Scan, (Y-Scan). For X-Scan (Y-Scan), the row and column of a matching position correspond to the x-coordinates (y-coordinates) of its current and previous frame's blocks, respectively. X-Scan (Y-Scan) show alignment of matching positions clearly, although the information of y-direction (x-direction) disappear in X-Scan (Y-Scan). Then, we solve the assignment problem on the original (not collected) cost matrix.

We assume that a CG synthesized object is moving, and we calculate its screen coordinates to show the alignment of the matching positions. We show the simulation results of the X-Scan and Y-Scan pattern when an object moves to the right in Fig. 7, and when an object approaches the camera in Fig. 8. Different colors are assigned to the matching positions according to the face to which the corresponding block belongs. We see that the matching positions are arranged approximately on lines for both X-Scan and Y-Scan.

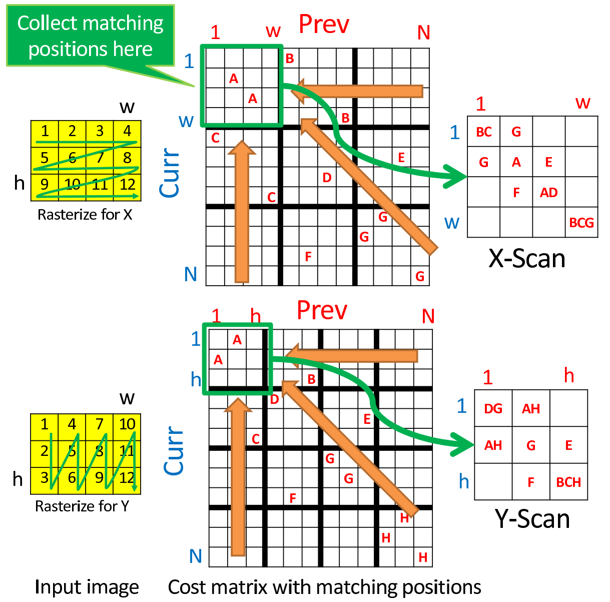

Fig. 6 Generation of X-Scan and Y-Scan. Each letter in the cost matrix means matching position and corresponds to the same letter in the X-Scan (Y-Scan).

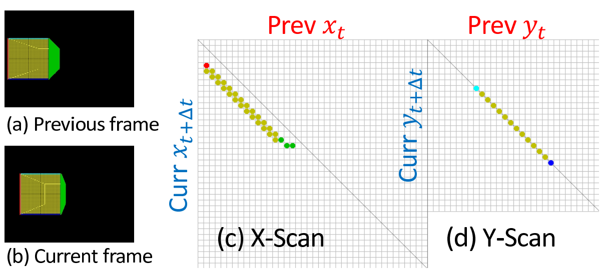

Fig. 7 X-Scan and Y-Scan for an object moving right.

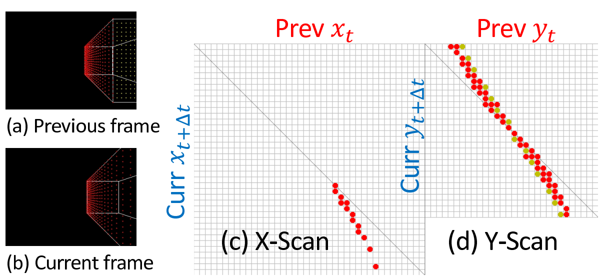

Fig. 8 X-Scan and Y-Scan for an object approaching the camera.

In other words, all the matching points of an object satisfy the same relational expression between their x-coordinates (y-coordinates) in the current and previous frames, and the relational expression is approximately linear. In the following, we discuss the relational expression that is satisfied for two kinds of basic movement: parallel displacement and rotation in the world coordinate.

We define that $\mathbf{X}_t = [X_t\ Y_t\ Z_t\ 1]^T$ is the world coordinate of a point q at time t, $\mathbf{x}_t = [h_t x_t\ h_t y_t\ h_t\ 1]^T$ is the screen coordinate that corresponds to q, P is a projection matrix, and $PA = P[R|\mathbf{t}]$ is a perspective projection matrix. That is,

$$\mathbf{x}_t = PA\mathbf{X}_t. \tag{2}$$

For ease of explanation, we assume that the camera position is fixed at the origin of the world coordinate, the camera angle does not vary ($A = I$), and

$$P = \begin{bmatrix} f & 0 & 0 & 0 \\ 0 & f & 0 & 0 \\ 0 & 0 & 1 & 0 \\ 0 & 0 & 0 & 1 \end{bmatrix}, \tag{3}$$

where f is the focal distance. From Eq. (2), the screen coordinate x_t, y_t can be expressed as

$$x_t = \frac{fX_t}{Z_t}, \tag{4}$$

$$y_t = \frac{fY_t}{Z_t}. \tag{5}$$

Here, we denote the time of the previous frame by t and the time of the current frame by $t + \Delta t$. We assume that Δt is sufficiently small. The screen coodinate of current frame can be expressed as:

$$x_{t+\Delta t} = x_t + \frac{dx_t}{dt}\Delta t; \tag{6}$$

$$y_{t+\Delta t} = y_t + \frac{dy_t}{dt}\Delta t. \tag{7}$$

Therefore, we can obtain the correspondence between current frame and previous frame by calculating of the screen coordinates x_t, y_t and its time derivative dx_t/dt, dy_t/dt.

Here, an object is composed of multiple points. We consider that many points on the object move at the same time. Then, their matching positions form a certain figure on the cost matrix. We assume that an object is a cuboid. X_t, Y_t, Z_t have ranges represented by

$$\begin{cases} X_a \le X_t \le X_b, \\ Y_a \le Y_t \le Y_b, \\ Z_a \le Z_t \le Z_b. \end{cases} \tag{8}$$

$\mathbf{X}_t$ is expressed by

$$\mathbf{X}_t = B(t)\mathbf{X}_0, \tag{9}$$

where, $\mathbf{X}_0 = [X_0\ Y_0\ Z_0\ 1]^T$ is the location at time $t = 0$, and $B(t)$ is the affine transformation that includes translation and rotation.

(1) Parallel displacement

Assuming that the movement of the object constitutes only parallel displacement, we can write

$$B(t) = \begin{bmatrix} 1 & 0 & 0 & v_x t \\ 0 & 1 & 0 & v_y t \\ 0 & 0 & 1 & v_z t \\ 0 & 0 & 0 & 1 \end{bmatrix}, \tag{10}$$

where v_x, v_y, and v_z are the moving velocity of the object for the X, Y, and Z axis, respectively.

By substituting Eq. (10) into Eq. (9), point $\mathbf{X}_t = [X_t\ Y_t\ Z_t\ 1]^T$ is represented as

$$\begin{bmatrix} X_t \\ Y_t \\ Z_t \end{bmatrix} = \begin{bmatrix} X_0 + v_x t \\ Y_0 + v_y t \\ Z_0 + v_z t \end{bmatrix}. \tag{11}$$

From Eqs. (4) and (5), x_t and y_t are written as

$$x_t = \frac{(X_0 + v_x t) f}{Z_0 + v_z t}, \tag{12}$$

$$y_t = \frac{(Y_0 + v_y t) f}{Z_0 + v_z t}. \tag{13}$$

Substituting these into Eqs. (6) and (7), we obtain

$$x_{t+\Delta t} = x_t + \Delta t \left(\frac{f v_x}{Z_t} - \frac{f X_t v_z}{Z_t^2} \right), \tag{14}$$

$$y_{t+\Delta t} = y_t + \Delta t \left(\frac{f v_y}{Z_t} - \frac{f Y_t v_z}{Z_t^2} \right). \tag{15}$$

First, we consider the points that have the same Z-coordinate as in the front face of the cuboid. Eliminating X_t and Y_t from Eqs. (14) and (15) using Eqs. (4) and (5), we obtain

$$x_{t+\Delta t} = \left(1 - \frac{v_z \Delta t}{Z_t}\right) x_t + \frac{f v_x \Delta t}{Z_t}, \tag{16}$$

$$y_{t+\Delta t} = \left(1 - \frac{v_z \Delta t}{Z_t}\right) y_t + \frac{f v_y \Delta t}{Z_t}. \tag{17}$$

These equations show that the matching positions are located on a line on the cost matrix for the multiple points that have the same Z coordinate, because $x_{t+\Delta t}$ ($y_{t+\Delta t}$) and x_t (y_t) for the points satisfy the same linear expression.

Second, we consider the points that have the same X or Y-coorinate as in the side, top, and bottom faces of the cuboid. We transform these equations using Eqs. (4) and (5) as

$$x_{t+\Delta t} = \left(1 + \frac{v_x \Delta t}{X_t}\right) x_t - \frac{v_z \Delta t}{f X_t} x_t^2, \tag{18}$$

$$y_{t+\Delta t} = \left(1 + \frac{v_y \Delta t}{Y_t}\right) y_t - \frac{v_z \Delta t}{f Y_t} y_t^2. \tag{19}$$

$x_{t+\Delta t}$ and $y_{t+\Delta t}$ are represented as a quadratic function of x_t, y_t. A parabola appears on the X-Scan if the sample points have the same X-coordinate. Similarly, a parabola appears on the Y-Scan if the sample points have the same Y-coordinate. In particular, when the object is at a distance from the camera and its movement is sufficiently small, the parabola has a gentle curve. We can approximate the parabola by a line because of the quantization of blocks. Then, we calculate the condition of the object's moving speed and distance for linear approximation. We can rewrite Eqs. (18) and (19) as

$$x_{t+\Delta t} = a_x x_t + b_x + E_x, \tag{20}$$

$$y_{t+\Delta t} = a_y y_t + b_y + E_y, \tag{21}$$

where, a_x, b_x, a_y, and b_y are constant and E_x and E_y are non-linear terms.

We define max(.) and min(.) as its maximum and minimum value when X_t, Y_t, Z_t is in the range represented by Eq. (8), respectively. It is necessary that E_x and E_y satisfy the following equations for the linear approximation.

$$\max(E_x) - \min(E_x) < \frac{\delta}{2} \quad \text{and}$$
$$\max(E_y) - \min(E_y) < \frac{\delta}{2}, \tag{22}$$

where δ is the block size on the screen.

Thus, E_x and E_y of Eqs. (18) and (19) are

$$E_x = -\frac{v_z \Delta t}{f X_t} {x_t}^2, \tag{23}$$

$$E_y = -\frac{v_z \Delta t}{f Y_t} {y_t}^2. \tag{24}$$

Substituting Eqs. (4) and (5) and removing the screen coordinates, we obtain

$$E_x = -\frac{v_z \Delta t f X_t}{Z_t^2}, \tag{25}$$

$$E_y = -\frac{v_z \Delta t f Y_t}{Z_t^2}. \tag{26}$$

Therefore, from Eq. (22), the condition of linear approximation is

$$\left| \frac{v_z \Delta t f X_b}{Z_a^2} - \frac{v_z \Delta t f X_a}{Z_b^2} \right| < \frac{\delta}{2} \quad \text{and}$$
$$\left| \frac{v_z \Delta t f Y_b}{Z_a^2} - \frac{v_z \Delta t f Y_a}{Z_b^2} \right| < \frac{\delta}{2}, \tag{27}$$

here, we assume that $X_a, X_b, Y_a, Y_b, Z_a, Z_b > 0$.

We show an example of the conditions under which a figure formed by the matching positions becomes a line in the cost matrix. We devide the screen into 40×30 blocks. As shown in Fig. 9, we assume that a camera whose scene width is equal to the distance from camera. The angle of view is about 53.1 degrees. In this case, the scene width is 40δ, therefore, $f = 40\delta$. We assume that the moving object is a cube the length of the sides of which is 1 m. We define the range of the object we can see as $X_t = 5$ m, -0.5 m $\leq Y_t \leq 0.5$ m, 10 m $\leq Z_t \leq 11$ m. In this case, we see

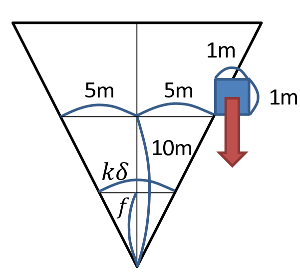

Fig. 9 The scene where we show the condition under matching positions align.

that the condition of linear approximation is $|v_z|\Delta t < 1.25$ m.

(2) Rotation around the X-axis and Y-axis

Here, we explain the matching position alignment for rotation around the Y-axis. For rotation around the X-axis can apply similar equations. When the object rotates around the Y-axis, we can write it using

$$B(t) = \begin{bmatrix} \cos\omega t & 0 & -\sin\omega t & 0 \\ 0 & 1 & 0 & 0 \\ \sin\omega t & 0 & \cos\omega t & 0 \\ 0 & 0 & 0 & 1 \end{bmatrix}, \tag{28}$$

where, ω is the rotation speed.

Substituting Eq. (28) into Eq. (9) and converting in a manner similar to that used for the parallel displacement, we obtain

$$x_{t+\Delta t} = x_t - \frac{\omega\Delta t}{f}x_t^2 - f\omega\Delta t, \tag{29}$$

$$y_{t+\Delta t} = y_t - \frac{\omega\Delta t}{f}x_t y_t. \tag{30}$$

This includes non-linear terms x_t^2 and $x_t y_t$. We adapt linear approximation in the same way as Eqs. (18) and (19).

Using Eqs. (4) and (5), the non-linear terms E_x and E_y of Eqs. (29) and (30) are written as

$$-\frac{\omega\Delta t}{f}x_t^2 = -\frac{\omega\Delta t f X_t^2}{Z_t^2}, \tag{31}$$

$$-\frac{\omega\Delta t}{f}x_t y_t = -\frac{\omega\Delta t f X_t Y_t}{Z_t^2}. \tag{32}$$

The condition under which matching positions align on a line is the same as Eq. (22), and we obtain the following condition.

$$\max\left(-\frac{\omega\Delta t f X_t^2}{Z_t^2}\right) - \min\left(-\frac{\omega\Delta t f X_t^2}{Z_t^2}\right) < \frac{\delta}{2} \quad \text{and}$$
$$\max\left(-\frac{\omega\Delta t f X_t Y_t}{Z_t^2}\right) - \min\left(-\frac{\omega\Delta t f X_t Y_t}{Z_t^2}\right) < \frac{\delta}{2}. \tag{33}$$

We show an example of conditions under which a figure formed by the matching positions becomes a line in the cost matrix. We consider the same object as that introduced in the example of parallel displacement. Here, we obtain $\max(X_t^2/Z_t^2) = 25/100$, $\min(X_t^2/Z_t^2) = 25/121$, $\max(X_t Y_t/Z_t^2) = 0.25/100$, and $\min(X_t Y_t/Z_t^2) = -0.25/100$. In this case, we see that the condition of linear approximation is $|\omega|\Delta t < 14.3$ deg.

(3) Rotation around the Z-axis

For the situation where the object rotates around the Z-axis, we can write

$$B(t) = \begin{bmatrix} \cos\omega t & -\sin\omega t & 0 & 0 \\ \sin\omega t & \cos\omega t & 0 & 0 \\ 0 & 0 & 1 & 0 \\ 0 & 0 & 0 & 1 \end{bmatrix}. \tag{34}$$

Substituting Eq. (34) into Eq. (9) and transforming it in the manner as that used for parallel displacement, we obtain

$$x_{t+\Delta t} = x_t - \omega\Delta t y_t, \tag{35}$$

$$y_{t+\Delta t} = y_t + \omega\Delta t x_t. \tag{36}$$

From this, we see that y_t is necessary for representing $x_{t+\Delta t}$ and x_t is necessary for representating $y_{t+\Delta t}$. Therefore, $x_{t+\Delta t}$ and $y_{t+\Delta t}$ are expressed by the following equations.

$$\begin{cases} x_{t+\Delta t} = ax_t + by_t + c \\ y_{t+\Delta t} = dx_t + ey_t + f \end{cases}. \tag{37}$$

These equations represent not a line but a plane in four-dimensional space. However, we call it an equation of a line to avoid confusion.

4. Solving Linear Assignment Problem to Satisfy Matching Position Constraint

In this section, we explain the method for obtaining the solution of the linear assignment problem that satisfies the matching position constraint. We solve the linear assignment problem using the Hungarian method [11]. The Hungarian method is executed as follows.

(1) Subtract the minimum value of each row from each element of the row.
(2) If we can choose n independent zeros (n: matrix size), which means every row and every column includes only one zero, the position of the zeros indicates the matching positions.
(3) Cover all zeros by the fewest possible horizontal or vertical lines.
(4) Subtract the minimum value of uncovered elements from them and add the value to the elements that are covered with both horizontal and vertical lines; go to (2).

Figure 10 shows an example of the Hungarian method for $n = 4$.

We can guess that the minimum value of each row tends to the solution of the assignment problem. They appear as zero-cost after we subtract the minimum value of each row from each element of the row. Therefore, if multiple zero-cost elements located on a line, we consider they

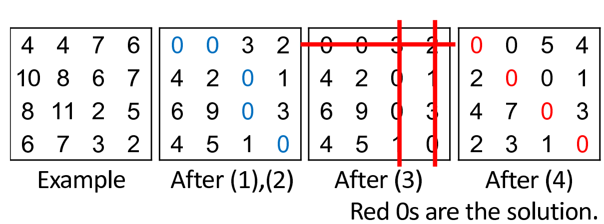

Fig. 10 Hungarian method.

are correct matching positions. For the proposed method, we extract lines including as many zero-cost elements as possible on the cost marix. We modify the values of the cost matrix based on the extracted lines.

Zero-cost elements that are on an extracted line and have no other zero-cost elements in the same row and same column must be determined as matching positions. We select them as a matching solution. By omitting them from the assignment, we can reduce the calculation time.

"Nonzero-cost elements on an extracted line" and "zero-cost elements near an extracted line" are considered to have been caused by the shape distortion of an object or an appearance change caused by an illumination change or reflection. We cannot distinguish whether or not the object has in fact transformed. This is the trade-off between the appearance change and shape change of the object. We should consider it an apperance change when the matching position is near an extracted line because the shape of an object does not change suddenly. Therefore, we decrease the cost of "non-zero elements on an extracted line" to raise the matching possibility. An element that is not on an extracted line and has low color similarity should not be a matching position. Therefore, we make its cost infinity so that it is not chosen.

The procedure of the proposed method is described below, and illustrated in Fig. 11.

(1) Subtract the minimum value of each row from each element of the row.
(2) On the cost matrix, extract the lines that cover as many zero-cost elements as possible using RANSAC [12].
(3) Mark the zero-cost element on the line as (a).
(4) Decrease the cost of non-zero elements on the line by Δc and mark as (b).
(5) An element the distance of which from the line is less than or equal to 1 and the color cost (distance) of which is less than a predefined threshold th is marked (c).
(6) Set the cost value of an element that is not marked as infinity.
(7) For each row that has only one marked element, if there is no marked element in the same column, determine the element as a matching position, and exclude the row from the assignment problem.
(8) Solve the assignment problem for the remaining rows using the Hungarian method.

We use RANSAC as a line extraction method. If the number of "zero-cost elements" that align on a continuous line is four and over, we consider them a meaningful line for the matching position constraint. The extracted lines should be continuous for 24 neighbor blocks on both X-Scan and Y-Scan.

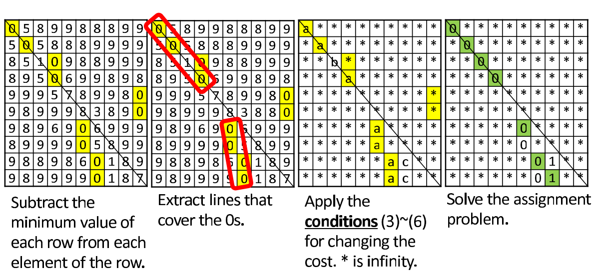

Fig. 11 Exclusive block matching with matching position constraint.

5. Experimental Results

We show the flow extraction results of the proposed method for static and moving camera images. The parameters in (4) and (5) of the proposed method procedure in Sect. 4 are fixed values. We set the value Δc in (4) is 50, and the value th in (5) is 50, which are one a ninth of Create (appearance of the new object) threshold 450, where similarity is normalized to 0 to 1000. We see that these values are not sensitive to scenes for these experiments.

A comparison of the results for the static camera images in Figs. 12 and 13 shows that the proposed method extracted more precise flows than exclusive block matching without matching position constraint. The results for a moving camera shown in Figs. 14 and 15 demonstrate that by applying the proposed matching position constraint, the flows are appropriately extracted. The moving object and

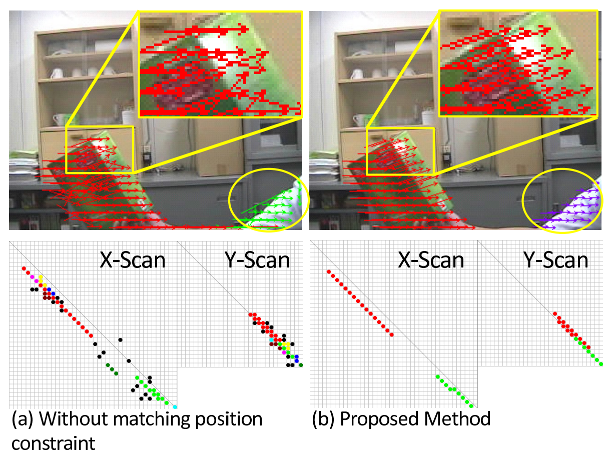

Fig. 12 Flow extraction for shifting box (static camera).

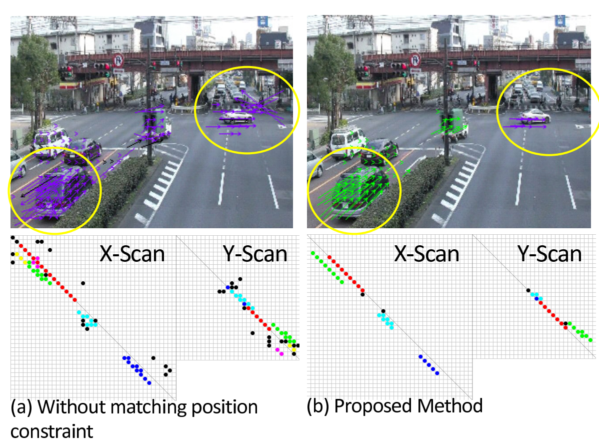

Fig. 13 Flow extraction for traffic intersection scene (static camera).

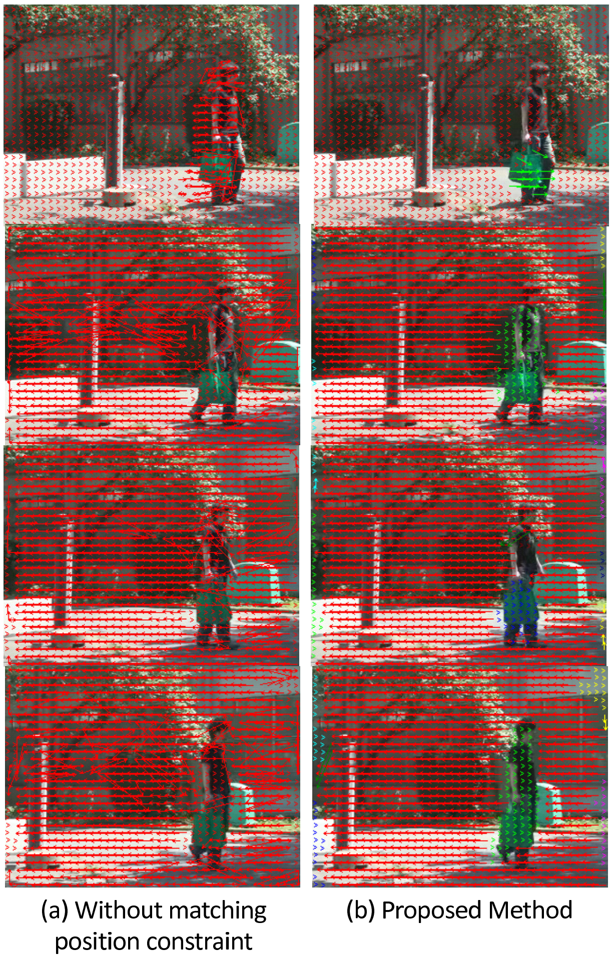

Fig. 14 Flow extraction for moving camera.

Fig. 15 Flow extraction for moving camera.

the background are separated appropriately by the flows.

We also show an appication for template matching. For template matching, instead of the previous frame, a template is used. The matching position constraints are applied as for object tracking. In Table 1, we compared the proposed method with six existing methods in [14]–[18], and [8] for David Indoor [19]. We define that matching is successful when all blocks of the template match to the target. The proposed method and the methods in [18] and [8] achieved the highest accuracy.

Moreover, in Table 2, we show a comparison with the method in [8] for six data including David Indoor. In these experiments, we also adopted Kalman Filter [13] to predict the object location. We reduced the cost of the blocks near the object position predicted by the Kalman filter. By using the Kalman Filter, the number of successful frames is improved for three data: David Outdoor, Sylvester, and Road Bridge. As compared with the method in [8], the proposed method realized more robust template matching. Examples of the template matching results are shown in Fig. 16. For template maching, both the method in [8] and the proposed method adopt HOG Context [8] as a block feature. As we see from the matching result in Fig. 16, the matching blocks

Table 1 Comparison with recent tracking methods in terms of the frame number after which the tracker does not recover from failure [8], [17], [18]. 761 means that tracking succeeded for all frames.

Frames	[14]	[15]	[16]	[17]	[18]	[8]	Proposed method
761	17	94	135	759	761	761	761

Table 2 Comparison of the number of successful frames using the method in [8] and the proposed method. Note that the meaning of the numbers on this table differ from that on Table 1.

Scene	Frames	GA [8]	Proposed method Without K.F.	Proposed method Using K.F.
David Indoor [19]	761	761	761	761
David Outdoor [19]	112	109	109	112
Sylvester [19]	1344	963	1299	1307
Car4 [19]	658	264	612	589
Backpacker	109	97	109	109
Road Bridge	63	60	59	63

preserve the shape of the target in the proposed method. Moreover, matching is succeeded in scenes David Outdoor and Sylvester that include the frame which has shaded target. It means that the matching position constraint is robust for illumination change. However, matching is failed

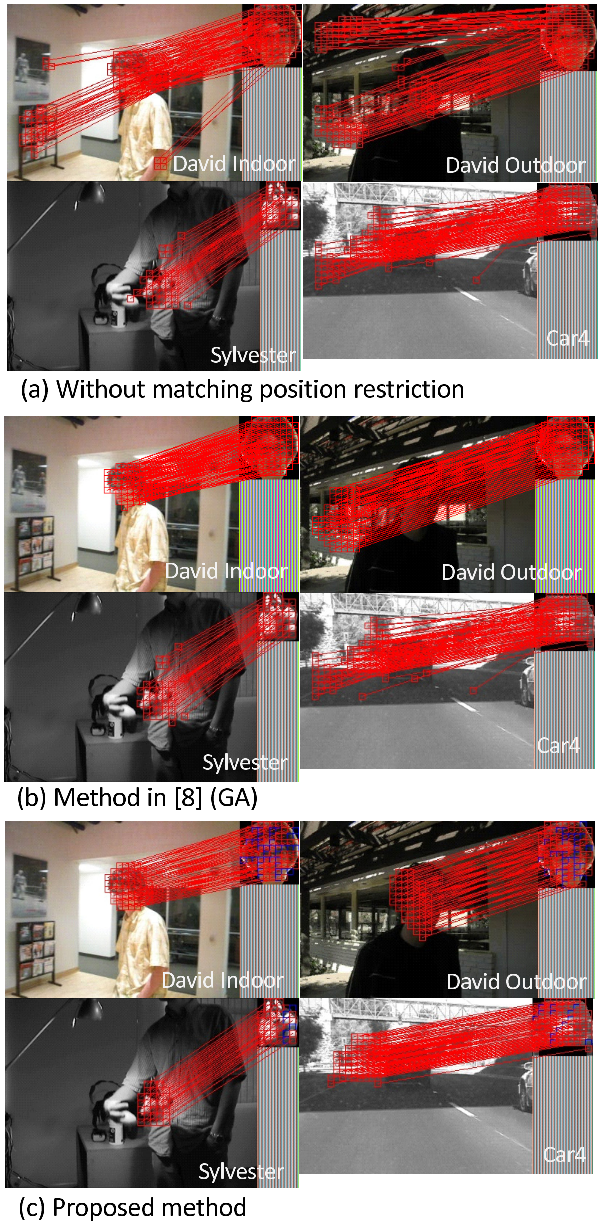

Fig. 16 Comparison of the result of template matching.

Table 3 Comparison of calculation time using the method in [8] and the proposed method.

David Indoor [s/frame]			
Without matching position constraint	GA	Proposed method Without K.F.	Proposed method Using K.F.
2.681	5.149	2.787	2.763

in scene Car 4. It is considered that illumination change is too strong.

In Table 3, we show the calculation time per frame for four methods: exclusive block matching without matching position constraint, the method in [8], the proposed methods with and without Kalman Filter. The calculation time of the proposed method is comparable with the original exclusive block matching, and it is shorter than that of the method in [8].

Table 4 Comparison of overlap ratio. "without MCP" is "matching position constraint".

scene	Without MCP	GA	Proposed method Without K.F.	Proposed method Using K.F.
David Indoor	0.716	0.747	0.750	0.735
David Outdoor	0.604	0.619	0.695	0.697
Sylvester	0.579	0.609	0.702	0.699
Car4	0.526	0.516	0.614	0.504
Backpacker	0.550	0.478	0.763	0.742
Road Bridge	0.660	0.655	0.684	0.687

Table 5 Comparison of average center location errors (pixel). "without MCP" is "matching position constraint".

scene	Without MCP	GA	Proposed method Without K.F.	Proposed method Using K.F.
David Indoor	13.07	9.09	7.07	7.07
David Outdoor	18.30	16.43	10.88	7.66
Sylvester	19.23	15.91	8.68	7.08
Car4	24.77	21.91	10.27	36.90
Backpacker	21.56	22.69	5.46	5.78
Road Bridge	15.98	15.59	14.10	12.68

Table 6 Comparison of number of success frames (Overlap ratio is greater than 0.5). "without MCP" is "matching position constraint".

scene	Without MCP	GA	Proposed method Without K.F.	Proposed method Using K.F.
David Indoor	629	670	704	679
David Outdoor	84	87	105	106
Sylvester	864	940	1207	1222
Car4	358	346	559	441
Backpacker	64	50	109	106
Road Bridge	48	49	58	59

We also evaluate the performance of the proposed method by Rui Yao's criteria [20]. We use the overlap ratio, center location error, and success frame for evaluation. Overlap ratio is defined as $R_{overlap} = Area(B_T \cap B_{GT})/Area(B_T \cup B_{GT})$, where B_T is the tracking bounding box and B_{GT} is the ground truth bounding box. If the overlap ratio is larger than 0.5, the matching is considered to be successful. We compare 'Without matching position constraint', 'GA', 'Proposed method' and 'Proposed method with K.F.'. The results are shown in Tables 4, 5, and 6. The proposed method generated more accurate results than without matching position constraint and GA.

6. Conclusion

We showed that the matching positions are located on a line on the cost matrix and that the method of calculation that retains the shape through exclusive block matching is effective. In the experiment, our method achieved more accurate tracking results in a shorter time than the previous method for static and moving camara images. For pratical application, we should improve the calculation time. This remains for future work.

References

[1] B.K.P. Horn and B.G. Schunck, "Determining optical flow," Artif. Intell., vol.17, no.1-3, pp.185–203, 1981.
[2] J.-Y. Bouguet, "Pyramidal implementation of the Lucas Kanade feature tracker," The paper is included into OpenCV distribution.
[3] D.G. Lowe, "Object recognition from local scale-invariant features," Proc. 7th IEEE International Conference on Computer Vision, vol.2, pp.1150–1157, 1999.
[4] Z. Li, K. Yabuta, and H. Kitazawa, "Exclusive block matching for moving object extraction and tracking," IEICE Trans. Inf. & Syst., vol.E93-D, no.5, pp.1263–1271, May 2010.
[5] Z. Li, Y. Tomioka, and H. Kitazawa, "Extraction and tracking moving objects in detail considering visual feature constraint and structure constraint," IEICE Trans. Inf. & Syst., vol.E96-D. no.5. pp.1171–1181, May 2013.
[6] T.S. Caetano, L. Cheng, Q.V. Le, and A.J. Smola, "Learning graph matching," Proc. 2007 IEEE 11th International Conference on Computer Vision, pp.1–8, 2007.
[7] R. Fletcher and M.J.D. Powell, "A rapidly convergent descent method for minimization," The Computer Journal, vol.6, no.2, pp.163–168, 1963.
[8] Z. Li, K. Tomotsune, Y. Tomioka, and H. Kitazawa, "Template matching method based on visual feature constraint and structure constraint," IEICE Trans. Inf. & Syst., vol.E95-D, no.8, pp.2105–2115, Aug. 2012.
[9] H. Jiang, M.S. Drew, Z.-N. Li, "Matching by linear programming and successive convexification," Proc. IEEE Trans. Pattern Anal. Mach. Intell., vol.29, no.6, pp.959–975, June 2007.
[10] N. Dalal and B. Triggs, "Histograms of oriented gradients for human detection," Proc. 2005 IEEE Computer Society Conference on Computer Vision and Pattern Recognition, vol.1, pp.886–893, 2005.
[11] H.W. Kuhn, The Hungarian Method for the Assignment Problem, Springer-Verlag Berlin, Heidelberg, 2010.
[12] M.A. Fischler and R.C. Bolles, "Random sample consensus: A paradigm for model fitting," Commun. ACM, vol.24, no.8, pp.381–395, 1981.
[13] G. Welch and G. Bishop, "An introduction to the Kalman filter," SIGGRAPH 2001, Course 8, 2001.
[14] J. Lim, D. Ross, R.S. Lin, and M.H. Yang, "Incremental learning for visual tracking," Advances in Neural Information Processing Systems, pp.793–800, 2004.
[15] S. Avidan, "Ensemble tracking," IEEE Trans. Pattern Anal. Mach. Intell., vol.29, no.2, pp.261–271, 2007.
[16] B. Babenko, M.-H. Yang, and S. Belongie, "Visual tracking with on-line multiple instance learning," Proc. 2009 IEEE Conference on Computer Vision and Pattern Recognition, pp.983–990, 2009..
[17] Q. Yu, T.B. Dinh, and G. Medioni, "Online tracking and reacquisition using co-trained generative and discriminative tracking," Computer Vision — ECCV 2008, Lecture Notes in Computer Science, vol.5303, pp.678–691, Springer Berlin Heidelberg, 2008.
[18] Z. Kalal, J. Matas, and K. Mikolajczyk, "P-N learning: Bootstrapping binary classifiers by structual constraints," Proc. 2010 IEEE Computer Society Conference on Computer Vision and Pattern Recognition, pp.45–56, 2010.
[19] Incremental Learning for Robust Visual Tracking, http://www.cs.toronto.edu/˜dross/ivt/
[20] R. Yao, Q. Shi, C. Shen, Y. Zhang, and A. van den Hengel, "Robust tracking with weighted online structured learning," Computer Vision — ECCV 2012, Lecture Notes in Computer Science, vol.7574, pp.158–172, Springer Berlin Heidelberg, 2012.

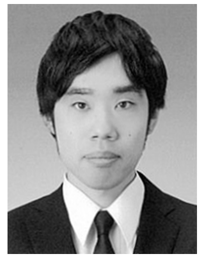

Tetsuya Okuda received his B.S. degree in Electrical and Electronic Engineering from Tokyo University of Agriculture and Technology, Japan, in 2013. He is currently pursuing a master's course at the university. His research interests include image processing.

Yoichi Tomioka received his B.E., M.E., and D.E. degrees from Tokyo Institute of Technology, Tokyo, Japan, in 2005, 2006, and 2009, respectively. He was a research associate at Tokyo Institute of Technology until 2009. He was an assistant professor in the Division of Advanced Electrical and Electronics Engineering at Tokyo University of Agriculture and Technology until 2015. Since 2015, he has been an associate professor in the School of Computer Science and Engineering at University of Aizu. His research interests include image processing, security systems with mobile robots, VLSI package design automation, and combinational algorithms. He is a member of IEEE and IPSJ.

Hitoshi Kitazawa received his B.S., M.S., and Ph.D. degrees in Electronic Engineering from Tokyo Institute of Technology, Tokyo, Japan, in 1974, 1976, and 1979, respectively. He joined the Electrical Communication Laboratories, Nippon Telegraph and Telephone Corporation (NTT), in 1979. Since 2002, he has been a professor at the Tokyo University of Agriculture and Technology. His research interests include VLSI CAD algorithms, computer graphics, and image processing. He is a member of IPSJ and IEEE.